



## Microemulsion-Based Topical Delivery of Coriander Essential oil: Formulation, Stability, and *In vivo* Evaluation for Delaying Skin Photoaging

ARUN KUMAR<sup>1\*</sup>, MAYUR PORWAL<sup>2</sup> and VAIBHAV RASTOGI<sup>2</sup>

<sup>1\*2</sup>Teerthanker Mahaveer College of Pharmacy, Teerthanker Mahaveer University, Moradabad-244001, Uttar Pradesh, India.

\*Corresponding author E-mail: arunsainibds@gmail.com

<http://dx.doi.org/10.13005/ojc/410529>

(Received: April 04, 2025; Accepted: October 01, 2025)

### ABSTRACT

Premature skin aging results from UVB and UVA radiation, leading to photoaging. Microemulsions facilitate efficient medication penetration into the skin via tiny droplets, as these small particles enhance permeation accessibility. This research paper aimed to produce and analyze coriander essential oil (CEO)-enriched microemulsions for topical application, along with their physical properties and *in vivo* anti-aging test outcomes. The CEO-based microemulsions, using Tween 80 as the surfactant, are prepared in conjunction with ethanol as the co-surfactant, incorporating CEO as the oil component. A comprehensive series of evaluations was performed on the formulations to determine their droplet size, zeta potential, pH, and viscosity, as well as to conduct TEM analysis, stability testing, and assess anti-aging efficacy through *in vivo* studies involving a UVB-exposed animal model. The optimized microemulsion droplets exhibited diameters ranging from 238 nm to 267 nm, pH values between 4.70 and 4.89, and viscosities between 75 and 90 cps. The droplet investigation using TEM revealed a uniform distribution of spherical forms. Histopathological findings indicated that microemulsion systems, which include CEO as an active component, safeguard ascorbic acid concentrations in skin tissue while concurrently reducing solar damage to dermal layers and organizing collagen networks. No signs of skin irritation were seen. CEO-loaded microemulsions displayed enhanced stability and provided substantial UVB protection, contributing to the mitigation of skin aging. The research results indicated that the Microemulsion (ME) based delivery system can effectively incorporate CEO into topical ME formulated for age reduction therapy. Future clinical research is necessary to evaluate the appropriateness of the CEO's approach in the cosmetic and dermatological product sectors.

**Keywords:** Microemulsion, Pseudo-ternary phase diagram, Photoaging, Coriander essential oil, UVB-Induced skin damage.

### INTRODUCTION

Both chronological and extrinsic factors influence the aging process of the skin. Most

skin aging is attributed to chronic exposure to environmental factors, including ultraviolet radiation from the sun, air pollution, and tobacco smoke. Photoaging is caused by sun radiation, including



infrared, ultraviolet A, and ultraviolet B rays, and visible light. DNA damage, genetic mutation, and the free radical theory are suggested causes of skin damage<sup>1</sup>.

Ultraviolet radiations (UV-R) are divided into three categories: 320–400 nm UVA, 280–320 nm UVB, and 200–280 nm UVC<sup>2</sup>. UV-A radiation causes immediate tanning, premature photoaging, suppresses immunologic functions, and leads to necrosis of endothelial cells. However, compared to longer wavelength radiation, UVB radiation damages connective tissue more effectively, resulting in skin roughness, wrinkles, and decreased elasticity. Skin wrinkles and drooping may arise from prolonged sun exposure that inhibits the production of collagen I, resulting in a reduction in the number of mature collagen bundles and an increase in the amount of immature collagen type III<sup>3</sup>. Microemulsions (ME) have gained appropriate attention in various fields because of their small particle size, deep penetration, long-lasting effects, and improved UV protection<sup>4</sup>.

Phytoconstituents, such as essential oils (EOs), are gaining prominence as ingredients in cosmetic formulations due to their potential to protect the skin against harmful agents and aid in treating various skin conditions<sup>5</sup>. EOs have demonstrated *in vitro* pharmacological activities in treating multiple diseases and have become a popular ingredient for skin care<sup>6</sup>. One common use of EOs in skin repair is that it can inhibit acne by inhibiting the proliferation of *Propionibacterium acnes*. Herbal extracts act on these areas, producing effects that include healing, softening, rejuvenation, and sun protection. For many years, phytochemicals have been utilized in cosmeceuticals; however, there are issues with the compounds' poor penetration and high instability in cosmetics. Small-droplet-size delivery methods are now utilized in the cosmeceutical industry to address these issues by providing sustained and improved delivery of plant-derived bioactive substances<sup>7</sup>.

## MATERIALS AND METHODS

### Ingredients

Tween 80 was purchased from CDH, India, and ethanol was obtained from Fisher Changshu Hongsheng Fine Chemical Co., Ltd. All other compounds and solvents used in this study were of scientific grade.

### Ethics declaration

The current study was conducted in accordance with ethical norms. The Institutional Animal Ethics Committee at Teerthanker Mahaveer Medical College and Research Centre, Moradabad, India, approved (Registration No. CCSEA/1205/2024/14).

### Preparation of coriander essential oil microemulsion

Coriander oil was used to create the ME, which was formulated with non-ionic surfactants, inert agents, such as Tween 80 (HLB 15), and deionized water. Due to Tween 80 elevated hydrophilic-lipophilic balancing value of 15, its utilization as a surfactant is advantageous<sup>8</sup>. Tween 80, as a non-ionic surfactant, employs steric stabilization to uphold the positioning of the microemulsion droplets. Tween 80 is categorized as a low-molecular-weight surfactant. Its low molecular weight was utilized in these microemulsions, reducing particle size and enhancing its efficacy in decreasing droplet size compared to polymeric surfactants.

### Development of microemulsions

#### Development of pseudo-ternary phase diagram (PTPD)

The water titration procedure was employed to construct the PTPD of ME at room temperature. The oil phase (CEO), the aqueous phase, the co-surfactant (ethanol), and Tween 80, which acts as a surfactant, were the four components of ME. A surfactant-co-surfactant mixture was formulated at varying weight ratios of 1:1, 2:1, and 1:2. The oil-to-smix ratio was altered in each phase diagram. Smix was incorporated into the oil phase within the test tube at weight percentages of 9:1, 8:2, 7:3, 6:4, 5:5, 4:6, 3:7, 2:8, and 1:9 % v/v (oil: Smix). Each test tube containing the combination was titrated incrementally with filtered water from a burette and mixed using a vortex shaker until turbidity was seen<sup>9</sup>. The necessary water volume was documented, and the percentage of each component was computed. The combinations were visually evaluated and categorized as ME or coarse emulsions. The phase diagram was generated with CHEMIX School Software<sup>10</sup>.

### Coriander essential oil-loaded microemulsion (ME)

The Development of a phase diagram serves as a proficient method for examining intricate interactions that may arise when various components

are amalgamated. Three microemulsion preparations of CEO were developed with differing quantities of the three elements. Smix was formulated utilizing a suitable ratio of Tween 80 and ethanol, and then combined with the CEO using a vortex shaker<sup>10</sup>. ME1, ME2, and ME3 were formulated with 25%, 20%, and 15% v/v of Smix, respectively, while the active phytoconstituents were employed in the form of CEO at a fixed ratio of 10%. After attaining homogeneity in the initial two compositions (water and Smix), a suitable amount of the drug (CEO) was incorporated at room temperature by agitating the mixes for 15 min to evaluate equilibrium. The three microemulsion preparations were analyzed for their physicochemical characteristics and assessed for their *in vivo* efficacy<sup>11</sup>.

#### **Characterization of prepared microemulsion Measurement of Zeta Potential and PDI**

Zeta potential and particle size were assessed using Malvern Instruments Ltd., UK Zetasizer, Version 7.10. A 5 mL sample was filtered using nylon membranes and then subjected to sonication for 10 minutes. Subsequently, 1-2 mL of the sample was transferred to the Zetasizer cuvette, and scanning was performed for 10 min, followed by data acquisition. The droplet potency or volume percentage (v/s) of the ME system was recorded. The polydispersity index, Z-average, and distribution estimations generated by a dynamic light scattering apparatus demonstrate these characteristics. These parameters affect many dimensions of the particle material, encompassing both quality and performance<sup>12</sup>.

#### **Determination of Viscosity and pH**

The temperature was constantly fixed at 25±1°C throughout the procedure. A Brookfield viscometer was subsequently used to assess the viscosity of the ME, with an average speed of 3 rpm per minute for a duration of 3 min, using spindle 61<sup>13</sup>. The pH of the microemulsions was analyzed utilizing a digital pH meter (Labtronics). The preparation was transferred to a beaker, and a pH meter was inserted into the solution; measurements were then documented<sup>14</sup>. The procedure was conducted thrice using identical formulas, and the average of the three measurements was determined as the pH. A similar method was utilized to ascertain the pH of all the microemulsions.

#### **Determination of Transmission Electron Microscopy**

TEM was employed to evaluate the bioerosion of the microemulsion droplets using the Thermo Scientific™ Talos L120C TEM. After applying a droplet of ME to a copper grid, the grid was stained for one minute using a 2% phosphotungstic acid solution. The grid was investigated at a 100 kV accelerating voltage. TEM is the paramount technology for reviewing the microstructures of microemulsions, as it immediately generates high-resolution images and can document co-existing structures and microstructural changes<sup>15</sup>. The appearance and structure of the microemulsions were analyzed using TEM. TEM studies involved applying a drop of the ME directly onto the holey film grid, and as it dried, the sample was studied<sup>16</sup>.

#### **Stability study**

The CEO microemulsion was maintained in stability chambers at temperatures of 5°C, 25°C, and 40°C with 75% relative humidity. The samples underwent physicochemical examination one week and one month after being stored under the specified stability conditions to assess the formulation's stability profile. Evaluations of appearance (including phase separation, color, and sedimentation), particle size, pH, viscosity, and polydispersity index (PDI) were conducted<sup>17</sup>.

#### **Assessment of thermodynamic stability**

We conducted two experiments to evaluate the thermodynamic stability of the prepared ME.

#### **Centrifuge-based stress assessment**

ME was subjected to centrifugation (Sisco) at 6,000 rpm for 30 min at 25±1°C, and thereafter examined for precipitation, flocculation, and phase separation.

#### **Freez-thaw stability evaluation test**

Each of the three complete freeze-thaw cycles applied to the ME included 24 h at 25°C and -5°C, and the samples were inspected for any change in their homogeneity<sup>18</sup>.

#### ***In vivo* anti-aging study**

##### **Measurement of ascorbic acid level (AA)**

To determine the amino acid composition, 1 g of skin tissue from every group was measured and subsequently crushed on a glass plate placed on ice, then blended. The homogenized tissue

was centrifuged at 8000 rpm for 10 min, and the supernatant was preserved in a deep freezer at  $-80^{\circ}\text{C}$  until the biochemical analyses began. A drop of thiourea, 1 mL of 2,4-dinitrophenyl hydrazine, and approximately 4 mL of tissue aliquots were utilized to initiate the reaction. The standard was 4 mL of AA solution ( $10\ \mu\text{g}/\mu\text{L}$ ), while the blank solution was 4 mL of 6% tricarboxylic acid. The experimental tubes were maintained in a water bath for 15 min and afterwards chilled. After that, 5 mL of sulfuric acid was incorporated into all tests and allowed to stand for 15 minutes. The optical density of all colored samples was assessed at 540 nm. The data were presented in mg of ascorbic acid /100 mL<sup>12</sup>.

### Skin irritation study

Wistar albino rats (150–200 g) were used to investigate the potential for skin irritation of the test compositions. Before the study, the rats were acclimated for seven days in a controlled laboratory environment. The study subjects were reserved in well-ventilated polypropylene cages with a temperature of  $25\pm 2^{\circ}\text{C}$  and a relative humidity of 60–90%. Standard laboratory feed and drinking water were supplied libitum<sup>12</sup>. The Institutional Animal Ethics Committee approved the study protocol following the rules established by the Committee for the Control and Supervision of Experiments on Animals. This study was approved under the approval number CCSEA/1205/2024/14.

Group 1: Control (no formulation administered)

Group 2: Administered formulation F1

Group 3: Administered formulation F2

Group 4: Administered formulation F3

The dorsal fur of each rat was shaved across an area of approximately  $25\times 25\ \text{mm}$ , and around 0.5 g of the test formulation was administered topically to the depilated location. The region was enveloped with a sterile cotton pad and affixed with adhesive tape. After 30 min, the area was gently washed with tap water to remove any remaining formulation. The treated skin areas were monitored for indications of dermal irritation, including erythema and edema, at 24 and 72 hours following application. Reactions were evaluated using a standardized scoring system for primary cutaneous irritation. Supplementary observations included alterations in skin color, shape, or texture throughout the observation period<sup>19</sup>.

### Assessment of efficacy against UVB-induced skin damage

Wistar albino rats were categorised into five groups ( $n = 6$ ). The rats were utilized to evaluate the photoprotective effectiveness of the test formulations against ultraviolet (UV)-induced dermal damage. All rats were shaved on their dorsal surface four days prior to the experiment to ensure uniform exposure to the test substance. A UV lamp generating radiation with a peak of 298 nm wavelength and a spectrum output ranging from 290 to 310 nm was utilized to produce photodamage. The radiation exposure dose (in  $\text{mJ}/\text{cm}^2$ ) was determined using the formula:

$$\text{Dose} \left( \frac{\text{mJ}}{\text{cm}^2} \right) = \text{Irradiance} \left( \frac{\text{mW}}{\text{cm}^2} \right) \times \text{Exposure time}(\text{min}) \times 60$$

The exposure procedure was established in compliance with OECD guidelines. Thirty minutes before each UV exposure, 2  $\text{mg}/\text{cm}^2$  of the test samples was administered topically to the depilated dorsal skin of the animals in Groups 3 (Gr-3), 4 (Gr-4), and 5 (Gr-5). The groups received a daily UV-radiation exposure of 500  $\text{mJ}/\text{cm}^2$  for 12 minutes over one month. The UV source was located 20 cm from the dorsal skin surface of the animals<sup>12</sup>.

Upon conclusion of the treatment period, the animals were euthanized, and the treated dermal regions were excised for histological examination. Skin samples were washed with physiological saline, fixed in 40% formalin, and preserved at  $-70^{\circ}\text{C}$  until subsequent processing.

Group 1: Control (no formulation administered)

Group 2: UVB-irradiated

Group 3: Formulation 1

Group 4: Formulation 2

Group 5: Formulation 3

### Histological Assessment

The dorsal skin tissue sections underwent hematoxylin and eosin staining for histological examination. A microscopic study was conducted to examine various parameters indicative of UV-induced skin damage. These encompassed epidermal thickness (to assess collagen fiber integrity and identify fragmentation or degradation in the dermis), inflammatory cell infiltration (presence of neutrophils, macrophages, or lymphocytes), edema (fluid accumulation), and sunburn cells

(apoptotic keratinocytes). Each attribute was semi-quantitatively evaluated using a standardized scale: (0-absent, 1-mild, 2-moderate, and 3-severe). The histology data were subsequently compared between the control and treatment groups to assess the protective efficacy of the test formulations against UV-induced skin damage<sup>12</sup>.

## RESULTS

### Pseudo-ternary phase diagrams construction

The Development of PTPD was utilized to ascertain the concentration variation in substances within the existence range of ME.

The transparent ME area was depicted in phase diagrams, with no clear transition from oil-in-water to water-in-oil ME seen. In the PTPD, one axis denotes the oil phase, another indicates the aqueous phase, and the third denotes the surfactant and co-surfactant mixture (Smix). The following ternary phase diagram shows PTPD for ME with various Smix ratios. The phase diagram having the highest ME region (isotropic region) was considered for further formulation optimization. Hence, it was found that a Smix ratio of 1:1 was selected for the preparation of ME, as shown in Fig. 1. The CHEMIX School software was employed to generate a PTPD.

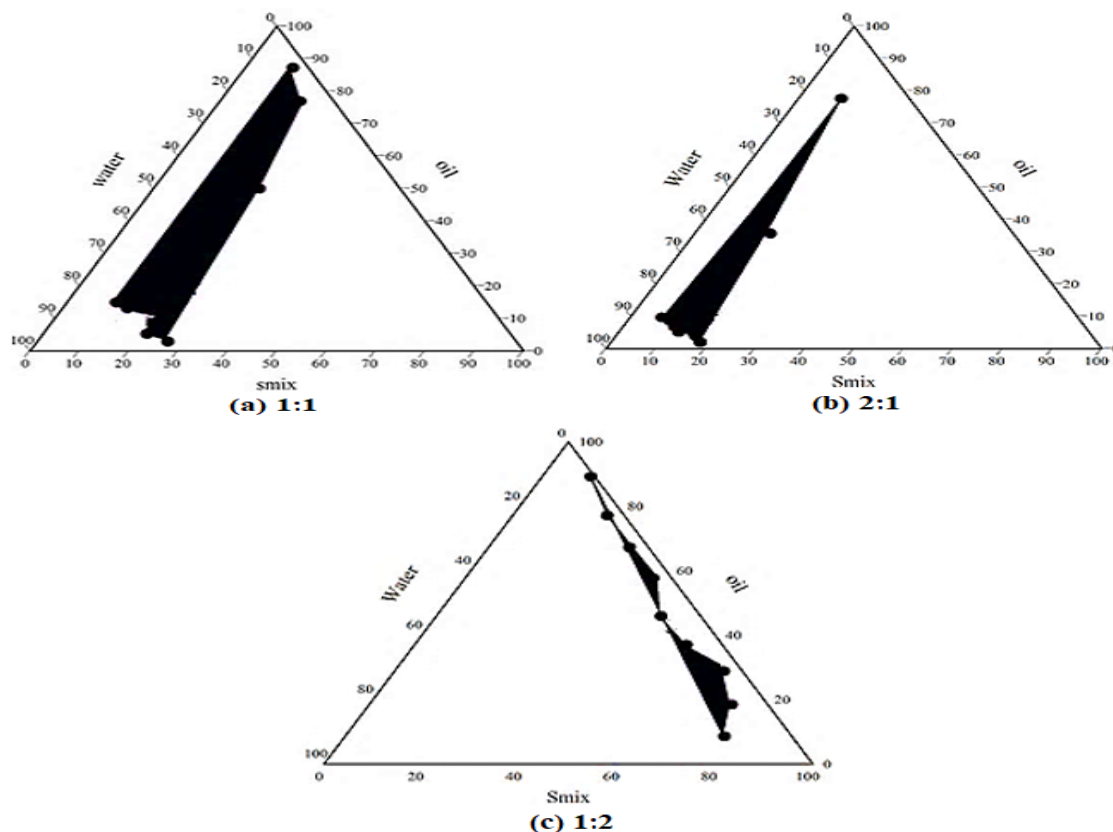


Fig. 1. Pseudoternary Phase diagram of CEO, Tween 80 & Ethanol consisting of varying Smix Ratios (a) 1:1, (b) 1:2, (c) 2:1

### Microemulsion Characterization

#### Measurement of zeta potential, & polydispersity index analysis

The Zeta potential of all formulations displayed in Table 2 was found to range from -1.07 mV to -1.79 mV, ensuring a decreased globule size and increased surface area. This improves the drug's skin penetration. According to Goindi *et al.*, (2013), the zeta potential of ME was found to be almost

neutral. The stability of microemulsions and lipid emulsions with non-ionic surfactants is independent of the zeta potential. The findings indicated that F2 exhibited the smallest particle size (17.47) relative to the other formulations. The polydispersity index of F1 was 0.334, which was nearer to 0 than the values of the different batches. The F1 batch had the lowest polydispersity index owing to the uniform distribution of globules in the formulation.

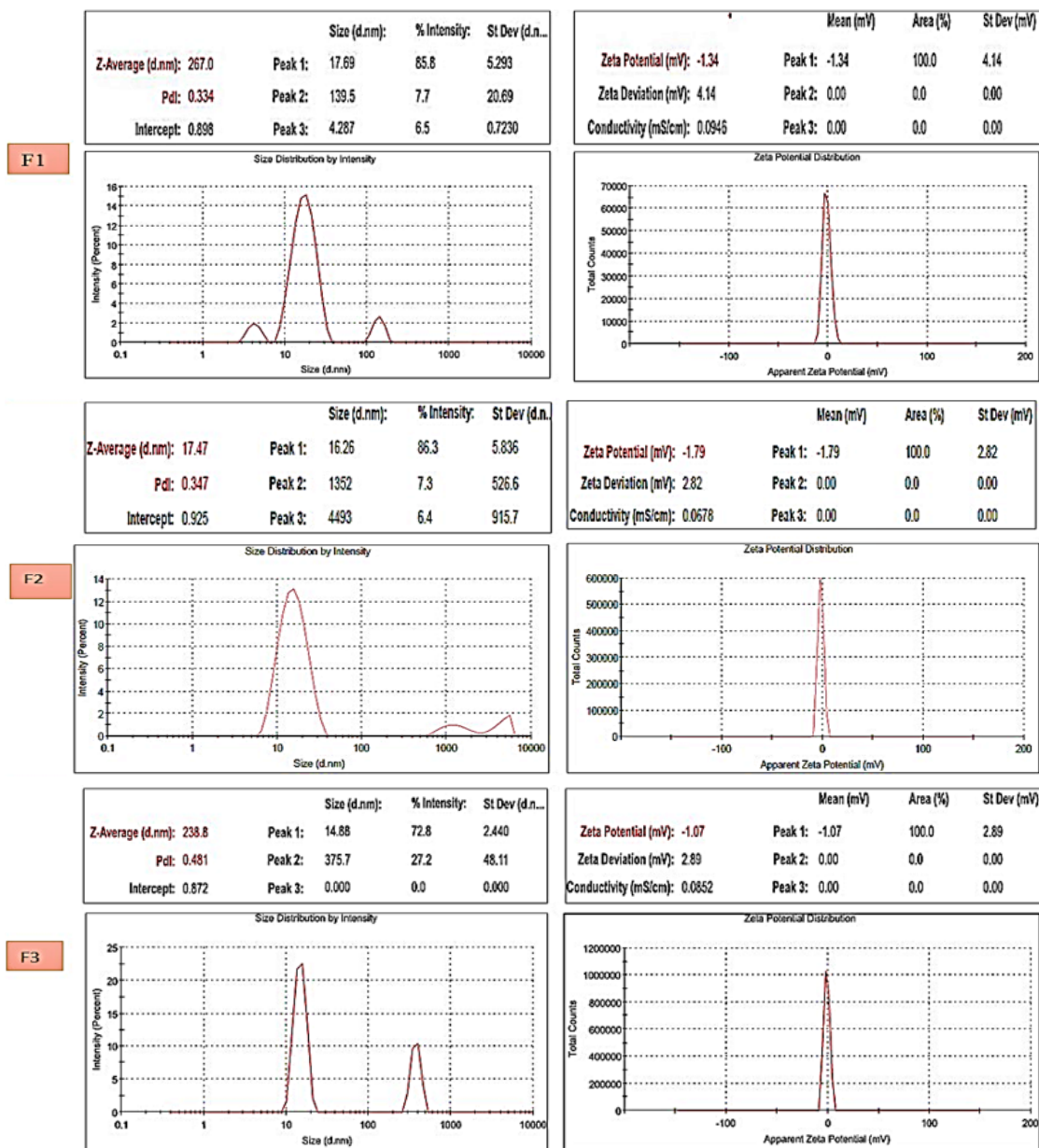


Fig. 2. F1, F2, and F3 formulations particle size and zeta potential characteristics

Table 1: Zeta potential and particle size of selected microemulsion formulations

Batch	Particle size (nm)	PDI	Zeta potential (mV)
F1	267	0.334	-1.34
F2	17.47	0.347	-1.79
F3	238.8	0.481	-1.07

**Viscosity**

All of the CEO-loaded ME had viscosity values between 90 and 75 cP. Increased viscosity values were observed for CEO-ME-1 90 in contrast with other CEO-loaded ME. The quantity of

surfactant in the ME certainly influenced the physical parameters, specifically the visible viscosity of the preparation. ME-3 exhibited a lower viscosity value of 75 cP. All prepared ME were within the appropriate range for topical application (Table 3). The viscosity of the microemulsions ranged between 90-75 cps, indicating that minimal shear forces readily dispersed the microemulsions

**pH**

The ME formulations appropriately

observed all the pH values best suited for topical application. Higher and lower concentrations of Smix did not considerably affect the noticed pH value of the microemulsion formulations. The pH of the CEO-loaded ME were mildly acidic, ranging from 4.70 to 4.89, which is highly well-matched with the natural pH of human skin (i.e., pH-4.7). Preparing skincare systems at a slightly lower pH (4–6) is advantageous. The pH and viscosity of the ME formulations, as represented in Table 3, were acceptable. The pH of all preparations ranged from 4 to 6, indicating a low possibility of skin irritation. All formulas exhibited clarity in appearance.

**Table 2: Evaluation parameters of microemulsion formulations**

Batch	pH	Viscosity (cps)	Thermodynamic stability
F1	4.89	90	Passed
F2	4.70	80	Passed
F3	4.70	75	Passed

### TEM study

TEM micrographs of the prepared formulations were obtained. The globule morphology of CEO-loaded ME is displayed in the above figures. The TEM images of F1 showed irregularity, while F2 and F3 revealed nearly spherical globule shapes with homogeneous droplet sizes. The homogeneous spherical droplets displayed in the photomicrographs exhibited a homogeneous distribution within the recommended range for ME systems and without agglomeration. The most common shape in microemulsions is spherical droplets, which often correspond to isotropic phases, such as W/O or O/W systems. These structures are formed due to the uniform distribution of surface-active substances (surfactants) at the droplet interface, which reduces the interfacial tension. Indicates a thermodynamically stable phase.

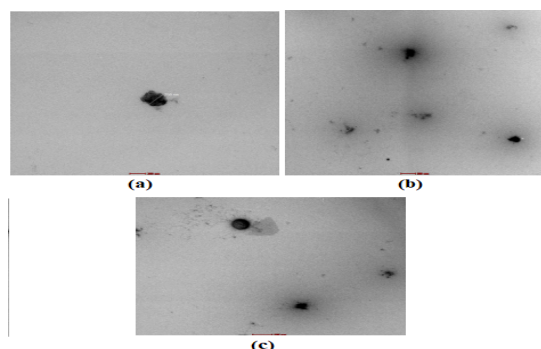


**Fig. 3. F1 Micrographs:** (a) TEM showed the size of globules of ME at the magnification of x17500 (scale bar showing 200 nm). b, and c) TEM of ME showed numerous globules of at the magnification of x6700 and 8500 (scale bar showing 500 nm)

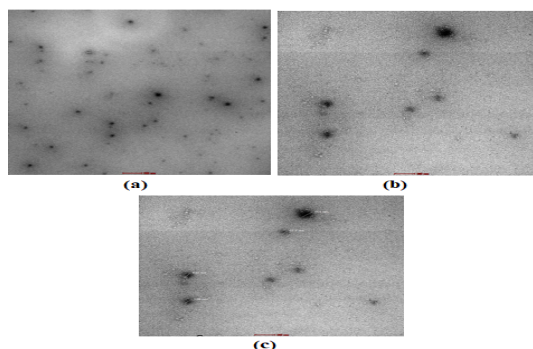


**Fig. 4. F2 Micrographs:** (a) 500nm and (b) 200nm 8500) TEM of ME showing numerous globules at the magnification of x8500 (scale bar showing 500 and 200 nm). (c) TEM showed the size of globules of ME at the magnification of x22000 (scale bar showing 200 nm)

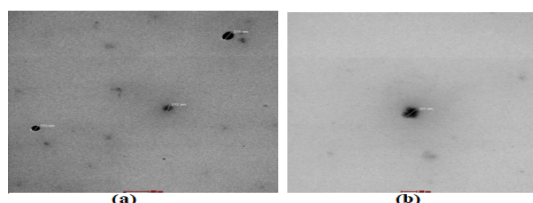


**Fig. 5. F3 Micrographs:** (a) TEM of ME showed numerous globule sizes, 500nm 11000 at the magnification of x11000 (scale bar showing 500nm). (b) TEM showed the size of globules of ME at the magnification of x17500 (scale bar showing 200 nm)

**Stability study:** The particle size was seen to be significantly different, however, still within the acceptable range. The results indicated that the formulation maintained stability after one month. Stability studies were conducted to investigate any changes in droplet size, pH, and physicochemical properties of the formulations after one month of storage at 40°C and 75% relative humidity. All preparations exhibited physical stability, maintaining homogeneity without phase separation after one month. Numerous skincare actives are susceptible to fluctuations in temperature, humidity, air exposure, and light. These environmental elements can readily deteriorate them, resulting in chemically unstable substances that compromise the effectiveness and safety of dermatological products. The standard method for assessing the roles of these actives involves monitoring alterations in physical features (Color change, precipitation, separation) as illustrated in Fig. 6 and Table 4. This study investigated the stability of CEO-loaded formulations under accelerated situations (40°C, 75% RH) for one month. ME were transparent after one month of storage.

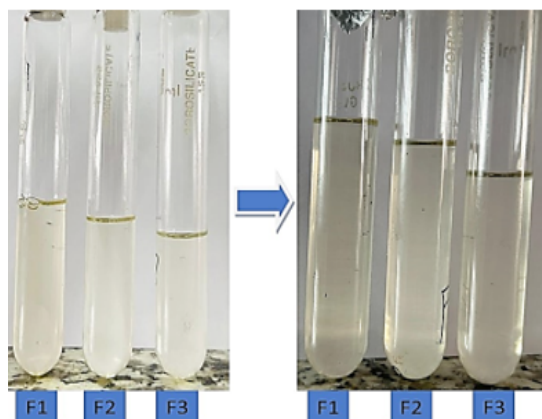


Fig. 6 (a) freshly prepared ME; stored at 40°C temperatures for 1 month: 1<sup>st</sup> week to last day of the month; [from left to right])

Table 3 Freshly prepared Microemulsions stability study

Parameter	1 <sup>st</sup> day			After 1 month		
	F1	F2	F3	F1	F2	F3
Viscosity(cps)	90	80	75	95	85	70
Particle size (nm)	267	17.47	238.8	336	63.51	177
Zeta Potential	-1.34	-1.34	-1.07	-3.022		
	-0.719					
	-1.871					
PDI	0.334	0.347	0.481	0.562	0.227	0.379
Ph	4.89	4.70	4.70	4.84		
	4.71	4.69				
Clarity	transparent	transparent	transparent	transparent	transparent	transparent

### Thermodynamic stability study

It was found that all ME formulations (F1, F2, F3) showed thermodynamic stability, without any phase separation, creaming, or cracking. ME demonstrated no breakdown, phase separation, or drug precipitation, which signifies thermodynamic stability against centrifugation and freeze-thaw cycles.

### *In-vivo* anti-aging study

#### Biochemical evaluation

The nonenzymatic parameter was employed to assess the AA level, elucidating the impact of CEO-based ME formulations on the skin's biochemical variables in Wistar albino rats subjected to UV radiation.

### Ascorbic acid estimation

Ascorbic acid is an essential component of the skin's defence and functions as a key nonenzymatic antioxidant in human tissues. While UVA or UVB rays do not absorb it and cannot be used as a sunscreen, it exhibits potent antioxidant qualities that safeguard the skin against UV-induced damage resulting from reactive oxygen species (ROS). The current study indicated that the AA concentration in group (Gr1) (Control) was  $5.71 \pm 0.14$  mg/mL, (AA, mg/100 ml Gr $\pm$ Std) while a significantly diminished AA concentration of  $1.88 \pm 0.14$  mg/mL was seen in Gr2, which was predominantly exposed to UVB radiation. Groups 3 ( $4.59 \pm 0.08$  mg/mL), 4 ( $5.40 \pm 0.05$  mg/mL), and 5 ( $5.4 \pm 0.05$  mg/mL) demonstrated markedly increased levels of AA following pre-treatment with CEO-loaded ME. The untreated group had a low AA level. The highest concentration of AA was observed in animals from groups 4 and 5, but a reduced amount was recorded in group 3, which received the CEO-loaded formulation.

### Skin irritation

The primary objective of the skin irritation study was to determine the degree of skin irritation caused by the preparation. A freshly created preparations ability to cause skin irritation is crucial for monitoring any localized, non-immunogenic inflammatory reaction that may arise locally and typically diminishes or resolves soon after application. Signs of skin irritation include pain, erythema, edema, and itching. These signals may indicate cellular, neurological, biochemical, or vascular responses to the onset of skin irritation. The formulation containing 10% v/v active ingredient (F3)

exhibited a primary irritation index of 0, indicating the best response. Formulations F1 and F2 showed PII values of 0.5 and 0.416, respectively, indicating slight irritancy. The results of the skin irritation test at both 24 and 72 h are presented in Table 5 and Figure 7.

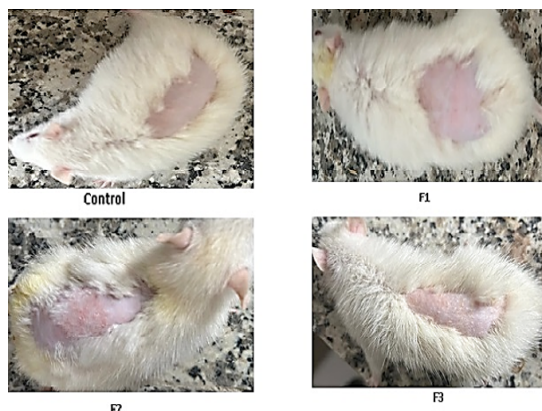


Fig. 7. *In vivo* skin irritation test for (F1, F2, F3) microemulsion: before application, and After application

Table 5 Primary irritation index of the microemulsion after 24 and 72 hours (n=6)

Formulation	Irritation index	
	24 h	72 h
Control	0	0
F1	0	0.5
F2	0	0.416
F3	0	0

### Histopathology

Mammals' epidermis is impacted by ultraviolet radiation, which accelerates the aging process of the skin. The adverse effects require investigations into the relationship between UV radiation and the skin. The purpose of this study was to use histological analysis to examine UV radiation affects the stratum corneum of the epidermis in Wistar albino rats. It was categorised into 5 groups (n = 6). Photomicrographs were analyzed after 30 days of treatment with the formulation in Gr-1 (Control, without exposure) and Gr-2 (with UV irradiation), which showed thick lines and wrinkles. The characteristics of UV-exposed skin in Gr-2 resembled those of chronic allergic contact dermatitis, exhibiting moderate to severe spongiosis. Groups 3 (Treatment F1 with UV irradiation), 4, and 5 (Treatments F2 and F3 with UV irradiation) demonstrated superior anti-wrinkle scores, as indicated by the arrow in the figure, compared to Group 3, with notably smoother and enhanced skin surfaces.

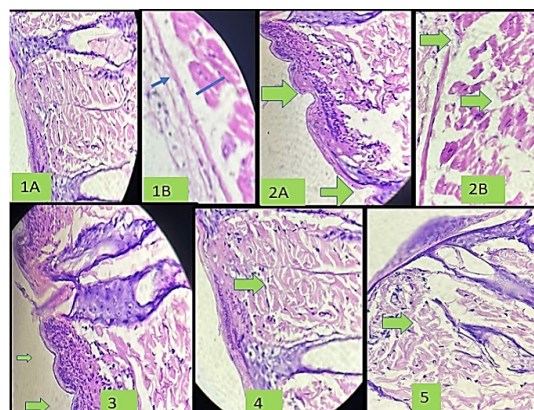


Fig. 8. Histopathological examination of skin parts from all the groups [1-A, B] the skin part of GP-1 [1-B, the line indicated the epidermis, and the arrow indicated the stratum corneum [2-A, B] Skin part of Gp-2 [2-B, the arrow indicated the epidermis, and in 2A represents the breakdown of stratum corneum and the damaged dermis]; (3) Skin part of Gp-3, (4) Skin part of Gp-4, (5) Skin part of Gp-5

The studied histological modifications revealed ultrastructural changes resulting from treatment and UV exposure. Histological analyses showed that collagen bundles suffered damage in Gr-2; however, well-structured collagen bundles were present in Gr-4 and Gr-5. The extent of collagen bundle disorganization increased in Gr-2, with further enhancement observed in Gr-4 and Gr-5 samples. There were notable similarities between the ultrastructural alterations in collagen fibers and those observed in UV-damaged skin. The level of collagen deterioration (Fig. 8) is illustrated in samples from the group exposed to ultraviolet radiation. The cellular composition of Gr-2 exhibited a thicker epidermis, likely because of the initial signs of photoallergic dermatitis and hyperkeratosis. Treatment with preparations in [Gr-3, Gr-4, and Gr-5] progressively decreased the liquefactive deterioration of the basal cell layer in the epidermal area. The histology of skin Gr-1 animals demonstrated normal connective tissue organization, but [Gr-3, -4, and -5] rats exhibited regenerative modifications in connective tissues, and decreased edema, suggesting evidence of significant UV exposure and subsequent dermal repair.

### DISCUSSION

ME were prepared via a spontaneous emulsification approach and optimization of several point parameters, including surfactant concentration, oil phase structure, and processing conditions. The results of the phase diagram indicated that a

stable ME zone was identified in the oil: Smix ratio, which includes a Smix ratio of 1:1. The choice of an appropriate surfactant is a crucial factor in developing an optimal ME formulation. Tween 80 was chosen for the ME formulation because it doesn't irritate the skin much, mixes well to create even droplets that are quickly absorbed and released, and has a low critical micelle concentration. Research indicates that an increase in surfactant concentration often results in a decrease in droplet particle size<sup>20</sup>.

The findings of microemulsions revealed low zeta potential. According to Hegde *et al.*, (2013), the minimal zeta potential observed differed from the traditional DLVO theory, recommending that specific non-DLVO forces significantly impacted the hydration of the surfactant head groups. It showed a small zeta potential of the ME after one month of stability testing, despite the ME displaying no obvious evidence of phase separation, flocculation, or instability. In summary, these non-DLVO forces, especially hydration interactions, affect stability and are essential in shaping how the colloidal system behaves when the zeta potential is different from what DLVO theory predicts. Deviates and is impacted by the hydration forces of surfactant head groups. By altering the surface characteristics of colloidal particles, such as the distribution of charge and the amount of water surrounding them, these hydration forces can significantly influence their behavior. Therefore, it is possible to modify the stability and behavior of colloidal microemulsions, particularly their zeta potential<sup>21</sup>.

The PDI is essential for assessing the stability of the ME preparation, which explores the distribution of a population's size within a particular sample.

In the current investigation, we discovered that the formulation was stable. This composition exhibits compatibility with skin and displays no irritating impact. From the above results, it is concluded that the formulated ME exhibited high consistency, homogeneity, and pH, and was non-greasy, with no phase separation observed over the study period. The formulations were stable. The results of TEM pictures reveal that CEO microdroplets were almost spherical in MEF3.

We observed a decrease in the ascorbic

acid level in skin tissues during UV radiation-induced injury. The groups of animals given CEO-loaded ME formulations (groups 4 and 5) had the highest amount of AA, indicating that these formulations help protect the skin from damage caused by UVB rays. The severity criterion for skin irritation adhered to a routine wherein scores below 0.5 indicated no irritation, values ranging from 0.5 to 3 denoted minor irritation, and ratings above 3 indicated severe irritation. The scores showed that none of the developed ME had any significant sensitivity reactions<sup>22</sup>. Overall, the application of the CEO-loaded ME resulted in minimal damage in the skin regions of groups 4 and 5. The CEO-loaded F2 (Gr-4) and F3 (Gr-5) ME formulations exhibited a more effective photoprotective effect than the F1 formulation.

The histopathological study aims to examine the impact of ultraviolet radiation on the stratum corneum of Wistar albino rats' skin by histopathological examination. The noted histological modifications indicated structural changes resulting from treatment and UV exposure. Histological studies revealed damage to collagen bundles in Gr-2, while Gr-1 showed well-organized collagen bundles. In Gr-3, the collagen bundles' disorientation was more compared to Gr-4 and Gr-5.

CEO-loaded ME demonstrated a reduction in wrinkles, improving skin elasticity. The antioxidants in coriander seed minimize UV-induced damage and therefore diminish skin aging. Its increased antioxidant abilities stem from its capacity to facilitate skin cell regeneration; hence, it maintains smooth skin, making it one of the most effective choices for anti-aging applications. Coriander seed oil also safeguards against skin damage from solar exposure and free radicals, while helping to reduce the appearance of scars and wrinkles in aging skin. This investigation revealed that the formulation can induce skin tightness, preventing skin damage and slowing down the aging process. It also showed a slight improvement in various elastic and viscoelastic characteristics; however, this improvement was not substantial. Our research was a preliminary step to uncover the positive benefits of coriander seeds, and further studies in this field should be conducted by adjusting the concentration of the extract in the formulation and by including volunteers who are elderly or experiencing skin problems<sup>23</sup>. Currently,

people require remedies for various types of skin-related diseases with minimal adverse effects. Herbal elements offer the possibility of developing cosmetic products with no adverse impact.

The results showed that adding the CEO to the microemulsion (ME) enhanced its protective properties, as it can penetrate deeper into the skin layers due to its smaller particle size compared to the F1 formulation. The results show that the CEO-loaded microemulsion (ME) formulations, especially F2 (Gr4) and F3 (Gr5), are very good at protecting the skin from harmful UV rays.

### CONCLUSION

External skin aging can be managed with the application of properly formulated and tested cosmetic products. This study investigates the potential of coriander seed oil cosmetic microemulsion (ME) against UV-induced skin damage and toxicity in Wistar albino rat skin. The antioxidants found in coriander seeds are known to repair damage caused by free radicals and prevent further harm. The photoprotective effectiveness of CEO-loaded ME formulations was assessed, revealing that pre-treatment with these formulations substantially mitigated adverse

biochemical alterations and safeguarded the skin against the harmful impacts of UVB radiation. The study's findings supported the anti-aging potential of the CEO and its photoprotective benefits. The Development and properties of ME containing CEO, recognized for its anti-aging benefits, were assessed. Additionally, the stability of ME was evaluated under various storage conditions, including time and temperature. This assessment ensures that the formulation maintains its efficacy and safety over time, a crucial requirement for practical applications. Such evaluations are essential for determining the product's shelf life and overall reliability in delivering its intended benefits. According to the research mentioned above, it can be stated that the CEO anti-aging ME is safe for use, as it is produced from herbal extracts.

### ACKNOWLEDGMENT

The authors express appreciation for the resources supplied by Teerthanker Mahaveer College of Pharmacy at Teerthanker Mahaveer University in Moradabad.

### Conflicts of interest

The authors disclosed no financial or other potential conflicts of interest in this study.

### REFERENCES

- Rastogi V.; Porwal M.; Sikarwar MS.; Kumar A. Phytoextract Loaded Nanoemulsions for Age-Defying Effects: A Review. *J Young Pharm [Internet]*, **2023**, *22*; 15(4), 604–15. Available from: <https://jyoungpharm.org/7297/>
- Wang J.; Chen Y.; He J.; Li G.; Chen X.; Liu H. Anti-Aging Effect of the Stromal Vascular Fraction/Adipose-Derived Stem Cells in a Mouse Model of Skin Aging Induced by UVB Irradiation., *Front Surg.*, **2022**, *9*.
- Souto EB.; Cano A.; Martins-Gomes C.; Coutinho TE, Zieli ska A, Silva AM. Microemulsions and Nanoemulsions in Skin Drug Delivery., *Bioengineering.*, **2022**, *9*(4), 1–22.
- Aziz ZAA.; Mohd-Nasir H.; Ahmad A.; Mohd. Setapar SH.; Peng WL.; Chuo SC., Role of Nanotechnology for Design and Development of Cosmeceutical: Application in Makeup and Skin Care., *Front Chem [Internet]*, **2019**, *13*; 7, 1–15. Available from: <https://www.frontiersin.org/article/10.3389/fchem.2019.00739/full>.
- Barradas TN, de Holanda e Silva KG. Nanoemulsions of essential oils to improve solubility, stability and permeability: A Review. *Environ Chem Lett.*, **2020**, *192* [Internet]. 2020 Nov 23 [cited 2023 Dec 5];19(2):1153–71. Available from: <https://link.springer.com/article/10.1007/s10311-020-01142-2>
- Guzmán E.; Lucia A. Essential Oils and Their Individual Components in Cosmetic Products., *Cosmetics [Internet]*, **2021**, *3*; 8(4), 114. Available from: <https://www.mdpi.com/2079-9284/8/4/114>
- Ganesan P.; Choi DK. Current application of phytocompound-based nanocosmeceuticals for beauty and skin therapy., *Int J Nanomedicine.*, **2016**, *11*, 1987–2007.
- Ghosh V.; Mukherjee A.; Chandrasekaran N. Ultrasonic emulsification of food-grade nanoemulsion formulation and evaluation of its bactericidal activity., *Ultrason Sonochem [Internet]*, **2013**, *20*(1), 338–44. Available from: <https://linkinghub.elsevier.com/retrieve/pii/S1350417712001782>

9. Patel TB, Patel TR, Suhagia BN. repairment, Characterization, and Optimization of Microemulsion for Topical Delivery of Itraconazole., *J Drug Deliv Ther.*, **2018**, 8(2), 136–45.
10. Rattanachitthawat N.; Rattanachitthawat S.; Peerakam N. Anti-Wrinkle Activity of Clausena harmandiana Essential Oil and Development of a Bioactive Nano-Drug Delivery System for Cosmetic Applications., *Pharmacogn J.*, **2022**, 14(4), 416–22.
11. El-Leithy ES.; Makky AM.; Khattab AM.; Hussein DG. Optimization of nutraceutical coenzyme Q10 nanoemulsion with improved skin permeability and anti-wrinkle efficiency., *Drug Dev Ind Pharm [Internet].*, **2018**, 44(2), 316–28. Available from: <https://doi.org/10.1080/03639045.2017.1391836>
12. Singh S.; Lohani A.; Mishra AK.; Verma A. Formulation and evaluation of carrot seed oil-based cosmetic emulsions., *J Cosmet Laser Ther [Internet].*, **2018**, 21(2), 99–107. Available from: <https://doi.org/10.1080/14764172.2018.1469769>
13. Mourya R.; Chauhan R. A Review on Marketed Formulations of Anti-Wrinkle Cream and Make an Effective Anti-Wrinkle Cream and Their Standardization., *Mourya at World J Pharm Res [Internet].*, **2019**, 8(7), 698. Available from: [www.wjpr.net](http://www.wjpr.net)
14. Lohani A.; Verma A.; Hema G.; Pathak K. Topical Delivery of Geranium/Calendula Essential oil-Entrapped Ethanolic Lipid Vesicular Cream to Combat Skin Aging., *Biomed Res Int.*, **2021**, 2021.
15. Chauhan L.; Muzaffar F.; Lohia S. Design, Development and evaluation of topical microemulsion., *Int J Pharm Pharm Sci.*, **2013**, 5(2), 605–10.
16. Shen LN.; Zhang YT.; Wang Q.; Xu L.; Feng NP. Preparation and evaluation of microemulsion-based transdermal delivery of total flavone of rhizoma arisaematis., *Int J Nanomedicine [Internet].*, **2014**, 9(1), 3453–64. Available from: <http://www.ncbi.nlm.nih.gov/pubmed/25092976>
17. Vinet L.; Zhedanov A. Microemulsion composed of combination of skin beneficial oils as vehicle: Development of resveratrol-loaded microemulsion based formulations for skin care applications., *J Phys A Math Theor [Internet].*, **2011**, 44(8), 1–14. Available from: <http://scioteca.caf.com/bitstream/handle/123456789/1091/RED2017-Eng-8ene.pdf?sequence=12&isAllowed=y%0A> [http://dx.doi.org/10.1016/j.regsciurbeco.2008.06.005%0Ahttps://www.researchgate.net/publication/305320484\\_SYSTEM\\_PEMBETUNGAN\\_TERPUSAT\\_STRATEGI\\_MELESTARI](http://dx.doi.org/10.1016/j.regsciurbeco.2008.06.005%0Ahttps://www.researchgate.net/publication/305320484_SYSTEM_PEMBETUNGAN_TERPUSAT_STRATEGI_MELESTARI)
18. Manognya JH. Design and Characterization of Microemulsion Systems for Etodolac., *World J Pharm Pharm Sci.*, **2017**, 3(1), 631–46.
19. Payyal SP.; Rompicherla NC.; Sathyanarayana SD.; Shriram RG.; Vadakkepushpakath AN. Microemulsion based gel of sulconazole nitrate for topical application., *Turkish J Pharm Sci.*, **2020**, 17(3), 259–64.
20. Eid AM.; Issa L.; Al-Kharouf O.; Jaber R.; Hreash F. Development of Coriandrum sativum Oil Nanoemulgel and Evaluation of Its Antimicrobial and Anticancer Activity., *Biomed Res Int.*, **2021**, 2021.
21. Hegde RR.; Bhattacharya SS.; Verma A.; Ghosh A. Physicochemical and pharmacological investigation of water/oil microemulsion of non-selective beta blocker for treatment of glaucoma., *Curr Eye Res.*, **2014**, 39(2), 155–63.
22. Chudasama A.; Patel V.; Nivsarkar M.; Vasu K.; Shishoo C. Investigation of microemulsion system for transdermal delivery of itraconazole., *J Adv Pharm Technol Res [Internet].*, **2011**, 2(1), 30. Available from: <https://journals.lww.com/10.4103/2231-4040.79802>
23. Akhtar N.; Zaman SU.; Khan BA.; Amir MN.; Ebrahimzadeh MA. Calendula extract: Effects on mechanical parameters of human skin., *Acta Pol Pharm-Drug Res.*, **2011**, 68(5), 693–701.